PACS numbers: 42.25.Dd; 42.25.Fx
DOI: 10.1070/QE2006v036n11ABEH013340

Angular structure of radiation scattered by a dispersed layer with a high concentration of optically soft particles

V.V. Berdnik, V.A. Loiko

***Abstract*. A method describing the propagation of radiation in concentrated dispersed media with optically soft particles is developed. The results of analysis of the angular structure of radiation scattered in the forward and backward semispheres depending on the direction of layer illumination, its optical thickness, concentration and the size of optically soft particles, are presented. The radiation transfer theory is used to describe the propagation of radiation. The radiation transfer equation is solved by the doubling method with the help of spline approximation averaged over the azimuth of scattering indicatrix in a unit volume. The parameters of the unit volume were determined by using the Mie theory and the interference approximation taking into account the collective scattering effects at a high concentration of particles.**

Keywords: *multiple scattering, concentrated dispersed media.*

1. Introduction

Scattering of radiation by natural and artificial media with a high particle concentration has been drawing the attention of researchers in recent years [1]. A rigorous description of scattering in close-packed media requires the use of the theory of multiple scattering of waves [2 – 5]. There are a number of effects that cannot be described by the conventional radiation transfer theory based on summation of intensities. Because of the complexity and cumbersomeness of the mathematical apparatus of the multiple scattering theory, complete solutions can be obtained in extremely rare situations. As a rule, publications devoted to analysis of the propagation of radiation in close-packed media are confined to an analysis of either the attenuation of a directed radiation beam [6, 7] or the angular structure of singly scattered radiation [8]. In most cases, such investigations are based on the equations of wave transport [9] and numerical simulation by the Monte Carlo method [10].

We have proposed a model of radiation transport in a layer of dispersed medium with a high concentration of optically soft particles [11, 12]. This model can be used for biological tissues, composite liquid crystal materials, polymer-dispersed liquid crystal films, liquated glasses, as well as porous glasses and structures.

This research is a continuation of the investigations started in [11, 12]. We shall present the results of analysis of the angular structure of radiation scattered in the forward and backward hemispheres, depending on the direction of illumination of the layer, its optical thickness, concentration and size of optically soft particles. During analysis, we took into account the optical interaction of particles associated with their spatial correlation and multiple scattering.

2. Model of radiation transport in a layer

Natural dispersed media with a high particle concentration usually have a considerable optical thickness. Multiple scattering effects should be taken into account during analysis of the characteristics of transmitted and reflected radiation.

Let an azimuthally symmetric wide radiation beam with intensity I_0 (Fig. 1) be incident at an angle θ_0 to the normal of a layer of a scattering medium confined from above and below by planes $z = 0$ and $z = z_0$. The scattering medium is a matrix with suspended monodisperse particles with radius R_p and a relative refractive index n_p. The refractive index n_m of the matrix is equal to the refractive index of the surrounding medium and hence there are no reflections at the boundaries. The radiation is scattered inside the layer, is partially absorbed and emerges from the layer through confining surfaces.

In order to describe the propagation of radiation in the layer, we use the radiation transfer equation (RTE) [13 – 17] which can be presented in the following form for an azimuth-averaged scattered radiation intensity when the layer is illuminated by a parallel radiation beam:

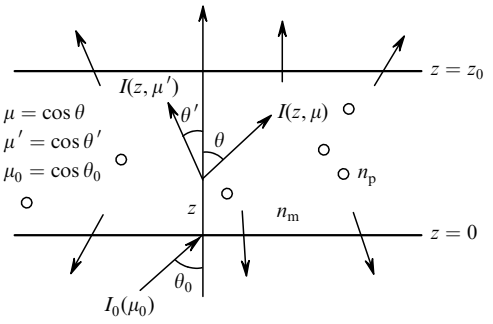

Figure 1. Schematic structure of a light-scattering layer.

V.V. Berdnik Institute of Aerospace Instrumentation, ul. Lipatova 2, Kazan, 420075 Russia; e-mail: vvberdnik@mail.ru;
V.A. Loiko B.I. Stepanov Institute of Physics, National Academy of Sciences of Belarus, ul. F. Skoriny 68, Minsk, 22072 Belarus; e-mail: loiko@dragon.bas-net.by

Received 30 June 2006; revision received 27 August 2006
Kvantovaya Elektronika **36** (11) 1016 – 1022 (2006)
Translated by Ram Wadhwa

$$\mu \frac{\partial I(z,\mu)}{\partial z} + \varepsilon I(z,\mu) = \sigma \int_{-1}^{1} p(\mu,\mu') I(z,\mu') \mathrm{d}\mu' + I_{1n}^{+} \sigma p(\mu,\mu_0) \times \exp\left(-\frac{\varepsilon z}{\mu_0}\right) + I_{2n}^{-} \sigma p(-\mu,\mu_0) \exp\left[-\frac{\varepsilon(z_0 - z)}{\mu_0}\right], \quad (1)$$

where $I(z,\mu)$ is the azimuth-averaged intensity of scattered radiation propagating inwards along the z axis at an axial angle $\theta = \arccos\mu$ to the direction of incident light; σ and ε are the scattering and attenuation coefficients; $\mu_0 = \cos\theta_0$; $p(\mu,\mu')$ is the azimuth-averaged phase function (redistribution function); $p(\cos\gamma)$ is the phase function in a unit volume, normalised by the condition $\int_{-1}^{1} p(\cos\gamma)\,\mathrm{d}\cos\gamma = 1$; $\cos\gamma = \mu\mu' + (1-\mu^2)^{1/2}(1-\mu'^2)^{1/2} \times \cos\varphi$; γ is the scattering angle; $\mu = \cos\theta$; $\mu' = \cos\theta'$; φ is the azimuthal scattering angle; I_{1n}^{+} and I_{2n}^{-} are the intensities of the directional radiation propagating into the layer, at the upper and lower boundaries respectively.

We solve the RTE with the following boundary conditions:

$$I(z=0,\mu>0) = I(z=0,\mu<0),$$
$$I(z=z_0,\mu<0) = I(z=z_0,\mu>0). \quad (2)$$

3. Calculation of the unit volume parameters

We begin the simulation of the parameters of close-packed media with their calculation in the low-concentration limit. In order to calculate the parameters of a unit volume in this limit, we use the Mie theory for spherical particles [18–20].

To calculate the attenuation coefficient and the phase function of a medium with a high particle concentration, we must solve the problem of diffraction of light from a many-body system. A rigorous solution of this problem has not been found so far, and hence various approximation methods are used to calculate the attenuation coefficient and the phase function. For weakly scattering particles, the interference approximation is the most convenient [7–10, 21–24]. According to this approach, the expressions for differential scattering coefficient $\sigma_{\mathrm{h}}(\gamma)$, scattering coefficient σ_{h}, and the attenuation coefficient ε_{h} for a medium consisting of identical spherical particles have the form

$$\sigma_{\mathrm{h}}(\gamma) = w\sigma_{0l} p_l(\gamma) S_3(\gamma, w), \quad (3)$$

$$\sigma_{\mathrm{h}} = w\sigma_{0l} u, \quad (4)$$

$$\varepsilon_{\mathrm{h}} = w(\varepsilon_{0l} - \sigma_{0l} + \sigma_{0l} u), \quad (5)$$

where

$$u = \int_0^{\pi} p_l(\gamma) S_3(\gamma, w) \sin\gamma\,\mathrm{d}\gamma; \quad (6)$$

$w = Nv/V$ is the volume concentration of the particles, N is the number of particles with volume v, contained in volume V of the medium; $\sigma_{\mathrm{h}}(\gamma)$ is the differential scattering coefficient of a medium with a volume concentration w of particles; σ_{h} and ε_{h} are the scattering and attenuation coefficients of a medium with a volume concentration w of particles; $\sigma_{0l} = \Sigma_{\mathrm{s}}/v$; $\varepsilon_{0l} = \alpha_{0l} + \sigma_{0l} = \Sigma_{\mathrm{e}}/v$; $\alpha_{0l} = \Sigma_{\mathrm{a}}/v$; Σ_{a}, Σ_{s} and Σ_{e} are the absorption, scattering and attenuation cross sections of an individual particle; and $p_l(\gamma)$ is the phase function of an individual particle normalised by the condition $\int_0^{\pi} p_l(\gamma)\sin\gamma\,\mathrm{d}\gamma = 1$.

The parameter u characterises the degree of optical interaction of particles. For independent scattering, its value is equal to unity. The stronger the correlation of particles in space, the larger the difference in the value of u from unity. Figure 2 shows how the value of u changes with the radius and concentration of uniform spherical particles for $n_{\mathrm{p}} = 1.05$. With increasing concentration of particles, the value of u decreases monotonically. The dependence on the radius, however, is not monotonic. Figure 3 shows the dependence of u on the refractive index and particle radius for $w = 0.5$. One can see that the peak value of u increases with decreasing the refractive index.

The structural factor $S_3(\gamma, w)$ takes into account the effect of light interference processes occurring in a system of correlated scatterers. For a system of rigid spheres, the structural factor is calculated in the Percus–Yevick approximation [7–10, 21, 22]:

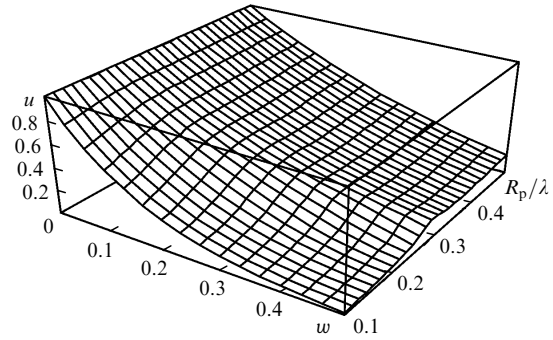

Figure 2. Dependence of u on w and R_{p}/λ for particles with $n_{\mathrm{p}} = 1.05$.

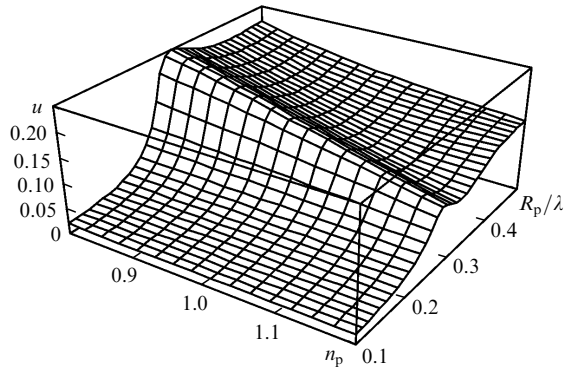

Figure 3. Dependence of u on n_{p} and R_{p}/λ for $w = 0.5$.

$$S_3(y,w) = \left(1 - 24w \int_0^1 c_3(x,w) \frac{\sin yx}{yx} x^2 \mathrm{d}x\right)^{-1}, \quad (7)$$

where $x = r/2R_{\mathrm{p}}$; r is the distance between two particles;

$$y = \frac{8\pi R_{\mathrm{p}}}{\lambda} \sin\frac{\gamma}{2}; \quad (8)$$

$$c_3(x,w) = -a - bx - cx^3; \quad (9)$$

$$a = \frac{(1+2w)^2}{(1-w)^4}; \quad (10)$$

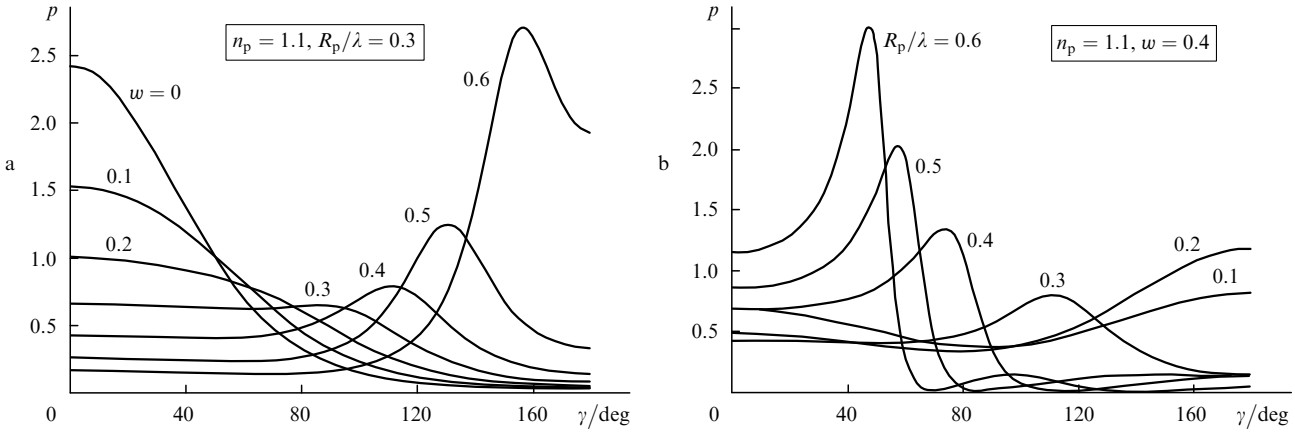

Figure 4. Dependence of the phase function of a unit volume on the concentration w (a) and radius R_p of particles (b).

$$b = -6w\,\frac{(1+0.5w)^2}{(1-w)^4}; \tag{11}$$

$$c = 0.5w\,\frac{(1+2w)^2}{(1-w)^4}. \tag{12}$$

Figure 4 illustrates the variation of the phase function upon a change in the concentration and size of the particles. The intensity of forward-scattered radiation decreases with increasing w and for quite high concentrations, the indicatrix acquires a characteristic maximum for a nonzero scattering angle. Upon an increase in the value of w, the maximum is displaced towards large angles, while an increase in the particle size displaces it towards small angles. Note that for certain values of the particle radius and concentration, the asymmetry $g = \int_{-1}^{1} p(\mu)\mu \mathrm{d}\mu$ of the indicatrix may be equal to zero, or even attain negative values (Figs 5 and 6).

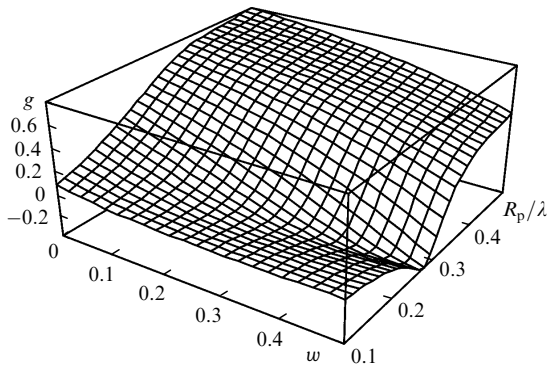

Figure 5. Dependence of the asymmetry parameter g on the concentration w and radius R_p of particles with $n_p = 1.1$.

It follows from expressions (4) and (5) that in the interference approximation, the absorption coefficient α_h is proportional to concentration ($\alpha_h = \varepsilon_h - \sigma_h = w\alpha_{0l}$). The optical thickness τ_0 of the layer, the single scattering albedo Λ, and phase function $p(\gamma)$ of the unit volume are defined by the formulas

$$\tau_0 = \tau_{0l}[1 - \Lambda_l(1-u)], \tag{13}$$

$$\Lambda = \frac{\Lambda_l u}{1 - \Lambda_l(1-u)}, \tag{14}$$

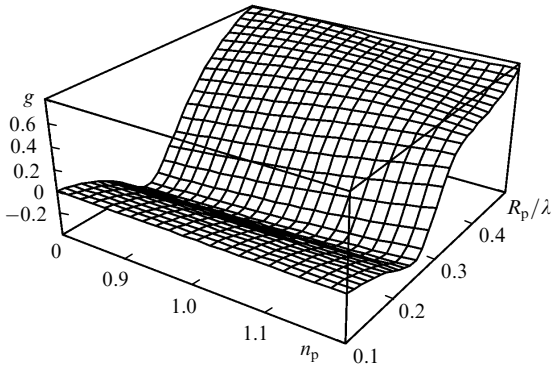

Figure 6. Dependence of the asymmetry parameter g on the refractive index n_p and radius R_p of particles for $w = 0.4$.

$$p(\gamma) = \frac{p_l(\gamma)S_3(\gamma)}{u}, \tag{15}$$

where τ_{0l} and Λ_l are the optical thickness of the layer and the single scattering albedo in the independent scattering approximation.

In order to solve the radiation transfer equation, we find the redistribution function

$$p(\mu,\mu') = \frac{1}{2\pi}\int_0^{2\pi} p\left(\mu\mu' + \sqrt{1-\mu^2}\,\sqrt{1-\mu'^2}\cos\varphi\right)\mathrm{d}\varphi. \tag{16}$$

This function is usually calculated by using series expansion in Legendre polynomials [14, 16]. For the phase functions having regions with clearly manifested peaks, however, several hundred terms in the expansion have to be taken into account, and the problem of calculation of the expansion coefficients p_l becomes complicated. If the number of expansion terms used in the calculations is not sufficient, the function $p(\mu,\mu')$ calculated from these coefficients acquires 'ripples' emerging as a result of incorrectness of the problem of summation of Fourier series with inaccurately defined coefficients. In this case, the redistribution function may acquire negative values.

In order to avoid these difficulties, we calculate $p(\mu,\mu')$ by using the spline approximation method [25, 26]. The use of splines helps in reducing the ripples due to their extremal properties (see [27], p. 147).

We use in the interval [–1, 1] a mesh of nodes q_i (i = 1, 2, ..., N) and approximate the indicatrix by a linear combination of base splines of nth order and defect $\Delta = 1$ [27]:

$$p(x) = \sum_{\alpha=1}^{N+n-1} B_\alpha(x) S_\alpha, \tag{17}$$

where $x = \cos\gamma$; $B_\alpha(x)$ are the base splines, and S_α is the spline vector.

Concentrating the nodes in the region of fast variation of the indicatrix, we can obtain a good approximation without increasing the number of nodes inordinately. Substituting relation (17) into (16), we obtain the following expression for the redistribution function:

$$p(\mu, \mu') = \sum_{\alpha=1}^{N+n-1} B_\alpha(\mu, \mu') S_\alpha, \tag{18}$$

where

$$B_\alpha(\mu, \mu') = \frac{1}{2\pi} \int_0^{2\pi} B_\alpha\Big(\mu\mu' + \sqrt{1-\mu^2} \times \sqrt{1-\mu'^2}\cos\varphi\Big) \mathrm{d}\varphi. \tag{19}$$

While calculating $B_\alpha(\mu, \mu')$, we have made the following change of variables:

$$x = \mu\mu' + \sqrt{1-\mu^2}\sqrt{1-\mu'^2}\cos\varphi.$$

In this case,

$$B_\alpha(\mu, \mu') = \frac{1}{\pi} \int_{N(\mu,\mu')}^{M(\mu,\mu')} \frac{B_\alpha(x)}{\{[M(\mu,\mu') - x][x - N(\mu,\mu')]\}^{1/2}} \mathrm{d}x, \tag{20}$$

where

$$M(\mu, \mu') = \mu\mu' + \sqrt{1-\mu^2}\sqrt{1-\mu'^2};$$

$$N(\mu, \mu') = \mu\mu' - \sqrt{1-\mu^2}\sqrt{1-\mu'^2}.$$

To evaluate the integral in Eqn (20), we used the Gauss quadratures [28] by introducing the Gaussian mesh

$$x_k = \mu v + \sqrt{1-\mu^2}\sqrt{1-\mu'^2}\cos\frac{k-0.5}{N_x}\pi, \quad k = 1, 2, \ldots, N_x \tag{21}$$

in the interval $[M, N]$, and replacing the integration by summation:

$$B_\alpha(\mu, \mu') = \frac{1}{N_x} \sum_{k=1}^{N_x} B_\alpha(x_k(\mu, \mu')). \tag{22}$$

The accuracy of this approximation technique was verified by considering the example of a medium with Heyney–Greenstein phase function for which the redistribution function is expressed through an elliptical integral of second kind. The error in the calculation of the function $B_\alpha(\mu, \mu')$ depends on the number of nodes N_x in the mesh x_k and is manifested in the errors of approximation of the phase function. The approximation error is the highest for $\mu = \mu'$, and decreases rapidly with increasing the distance from this point. The error increases with decreasing μ'. For an average cosine of the scattering angle $g < 0.96$, the maximum relative error does not exceed 2 % [25]. The highest stability to the variation of the medium parameters is attained when splines of the first order are used, i.e., if the indicatrix is approximated by a broken line.

4. Angular structure of scattered radiation

A homogeneous layer of a scattering and absorbing medium with nonreflective boundaries is characterised by the luminance factors of backward $[\rho(\mu, \mu')]$ and forward $[\sigma(\mu, \mu')]$ diffusely scattered radiation, which are defined by the relations

$$I^-(z = 0, \mu) = \int_0^1 2\rho(\mu, \mu')\mu' I_0(\mu')\mathrm{d}\mu', \tag{23}$$

$$I^+(z = z_0, \mu) = \exp\left(-\frac{\tau_0}{\mu}\right) I_0(\mu) + \int_0^1 2\sigma(\mu, \mu')\mu' I_0(\mu')\mathrm{d}\mu'. \tag{24}$$

Here, $I_0(\mu)$ is the intensity of radiation incident on the layer, $I^+(z, \mu) = I(z, \mu > 0)$ and $I^-(z, \mu) = I(z, \mu < 0)$ are the intensities of backward and forward radiation emerging from the layer.

The use of luminance factors in theoretical analysis and computational practice stems from their symmetry properties: $\sigma(\mu, \mu') = \sigma(\mu', \mu)$, $\rho(\mu, \mu') = \rho(\mu', \mu)$.

In order to determine the luminance factors $\rho(\mu, \mu')$ and $\sigma(\mu, \mu')$, we used a calculation approach based on the layer doubling technique [14, 16, 29–31]. In this method, the computations are started by choosing a layer of a quite small optical thickness τ_m so that $\tau_0 = \tau_m 2^K$, where K is an integer. For a layer with an optical thickness τ_m, the luminance factors are determined approximately. The methods of specifying approximate values of $\rho(\mu, \mu')$ and $\sigma(\mu, \mu')$ (initialisation) for isotropic media are defined in [30]. In the present paper, we have used single scattering initialisation. The luminance factors for a layer of doubled thickness were used with the help of familiar relations for layer doubling obtained from the balance equations at the layer boundaries [8, 10, 23, 24]. The initial optical thickness was assumed to be equal to $\tau_m \sim 10^{-6}$, which ensured a fairly high precision of the results of calculations.

Proceeding from expressions (23) and (24), we can write the expressions for the reflection (R) and transmission (T) coefficients as functions of the cosine μ_0 of the angle of incidence of radiation at the layer:

$$R(\mu_0) = 2\int_0^1 \rho(\mu, \mu_0)\mu\,\mathrm{d}\mu, \tag{25}$$

$$T(\mu_0) = \exp\left(-\frac{\tau_0}{\mu_0}\right) + 2\int_0^1 \sigma(\mu, \mu_0)\mu\,\mathrm{d}\mu. \tag{26}$$

If irregular node meshes are used for discretisation of layer summation equations, it becomes difficult to determine the calculation errors for phase functions having segments with sharply manifested peaks, but also for media with highly elongated phase functions. We estimated the error from the difference from unity of the sum of the coefficients of reflection $[R(\mu_0)]$ and transmission $[T(\mu_0)]$ of radiation incident at a layer with non-absorbing particles. We used a 150-point Gaussian quadrature on the interval $[0, 1]$. Cal-

culations show that this difference is small. For example, for a medium with particles having a refractive index $n_p = 1.01$ and an average radius $\bar{R}_p = 3.41$ μm, which was considered in [5], the departure from unity does not exceed 0.001.

Let us consider a few results of numerical analysis. The practice of analysis of light-scattering properties of dispersed layers in a close-packed state shows that the most interesting variations of light-scattering properties are observed for small particles with $R_p/\lambda = 0.05 - 0.5$. In this case, the scattering coefficient varies over a wide range, especially if the concentration effects are taken into account. Hence, the surface concentration of particles must be varied over a wide range while considering the laws of multiple scattering of radiation.

Figure 7 shows the phase functions of spherical particles with $R_p = 0.3$ μm and $n_p = 1.1$ for $\lambda = 0.5$ μm for $w = 0.001$ [curve (*1*), practically independent scattering] and $w = 0.5$ [curve (*2*)]. Figures 8 and 9 show the angular dependences of the luminance factors for layers with different overlapping coefficients (the overlapping coefficient is equal to the ratio of the area of projection of particle cross section to the area S of the surface on which they are located: $\eta = N\pi(R_p)^2/S$) for normal incidence of radiation. Upon an increase in η, and hence the optical thickness of the layer (the optical thickness τ_0 is proportional to the overlapping coefficient η), multiple scattering leads to smoothing of singularities of the phase function (the peak on the angular structure observed for small overlapping coefficients disappears), and the angular structure of scattered radiation does not change for quite large values of τ_0, which indicates a transition to the thickness regime.

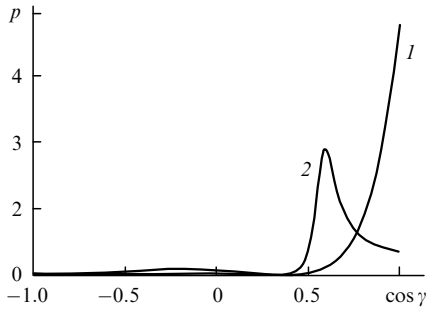

Figure 7. Phase functions of a unit volume of the medium formed by particles with $R_p = 0.3$ μm, $n_p = 1.1$ ($\lambda = 0.5$ μm) for $w = 0.001$ [curve (*1*)] and 0.5 [curve (*2*)].

One can see from Fig. 9 that upon an increase in η, the angular dependence of forward-scattered radiation displays a peak whose amplitude increases to its maximum value, after which it disappears for large values of η upon a transition to the thickness regime. Such a behaviour is a consequence of the characteristic peak in the phase function of a close-packed medium. Note that similar peculiarities may be displayed by the phase function of individual drops in a liquid crystal with bipolar and radial structures [32]. Part of the radiation incident on the layer is scattered at an angle $\theta = \gamma_m$ (γ_m is the angle at which the peak of the phase function is formed), while another part is scattered again at an angle γ_m and propagates in the direction of the incident light. Apparently, the formation of a peak in the forward scattered radiation takes place in the case when the

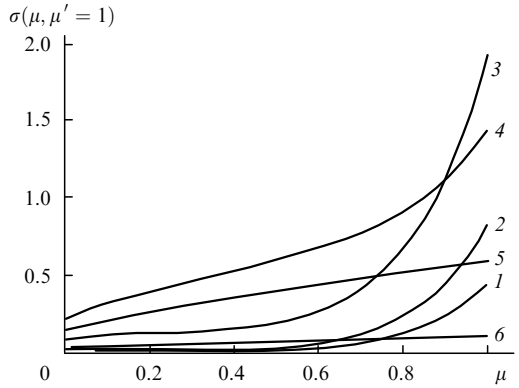

Figure 8. Luminance factors of a layer formed by particles with $R_p = 0.3$ μm, $n_p = 1.1$ ($\lambda = 0.5$ μm) and $w = 0.001$, for $\eta = 0.49$ [curve (*1*)], 0.98 [curve (*2*)], 3.91 [curve (*3*)], 15.63 [curve (*4*)], 62.5 [curve (*5*)], and 500 [curve (*6*)]; $u = 0.16161$, $\tau_{0l} = 131.26$.

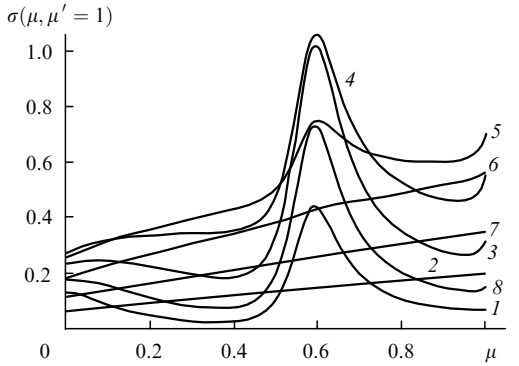

Figure 9. Luminance factors of a layer formed by particles with $R_p = 0.3$ μm, $n_p = 1.1$ ($\lambda = 0.5$ μm) and $w = 0.5$, for $\eta = 3.91$ [curve (*1*)], 7.81 [curve (*2*)], 15.63 [curve (*3*)], 31.25 [curve (*4*)], 62.5 [curve (*5*)], 125 [curve (*6*)], 250 [curve (*7*)], and 500 [curve (*8*)]; $u = 0.16161$, $\tau_0 = 21.5477$.

contribution from double scattering to the total intensity of scattered radiation is quite large. The intensity peak in the region of small angles of scattering is observed experimentally upon an increase in the particle concentration [5].

Angular dependences of the luminance factors $\sigma(\mu, \mu')$ are shown in Fig. 10 for various angles of incidence. Upon an increase in the incidence angle (decrease in μ'), the characteristic peak in the angular dependence of scattered radiation becomes blurred. Two peaks can be formed, the separation between them increasing with decreasing μ'. An analogous peak, but strictly in the backward direction, can be formed if the phase function of the unit volume has a peak at an angle of 90°. Figure 11 shows the phase function of a unit volume for such a medium. In the example considered by us, the medium contains particles with $R_p = 0.199$ μm and $n_p = 1.05$ ($\lambda = 0.5$ μm), the volume concentration of the particles being $w = 0.5$. For comparison, Fig. 11 also shows the phase function of the unit volume in the low concentration limit ($w = 0.001$). The angular dependences of the luminance factors of such layers with increasing thickness are shown in Fig. 12. A comparison of Figs 12a and b shows that layers with a concentration $w = 0.5$ are characterised by the formation of a peak in the strictly backward direction. No such peak is observed for low concentrations. Figure 13 shows the angular dependences of the luminance factor $\rho(\mu, \mu')$ of

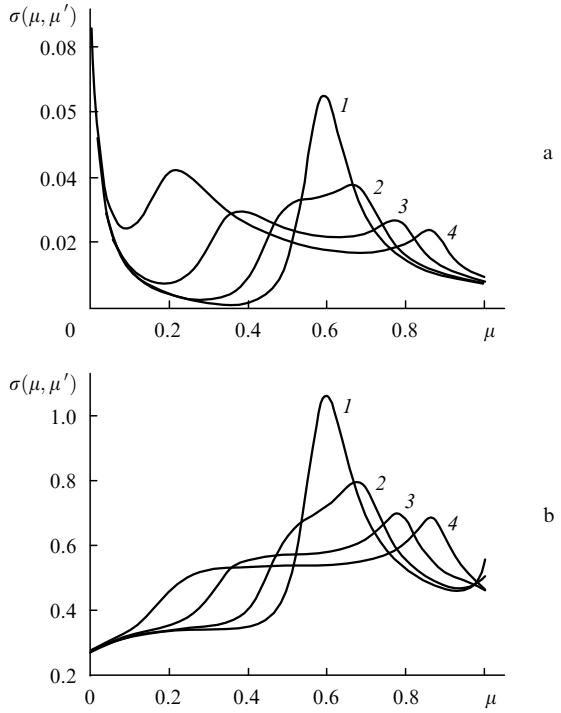

Figure 10. Angular dependences of the luminance factors $\sigma(\mu, \mu')$ of a layer formed by particles with $R_p = 0.3$ μm, $n_p = 1.1$ ($\lambda = 0.5$ μm) and $w = 0.5$, for $\mu' = 1$ [curve (*1*)], 0.99 [curve (*2*)], 0.96 [curve (*3*)], and 0.91 [curve (*4*)]; $u = 0.16161$, $\tau_{0l} = 131.26$, $\eta = 0.488$ (a) and 31.25 (b).

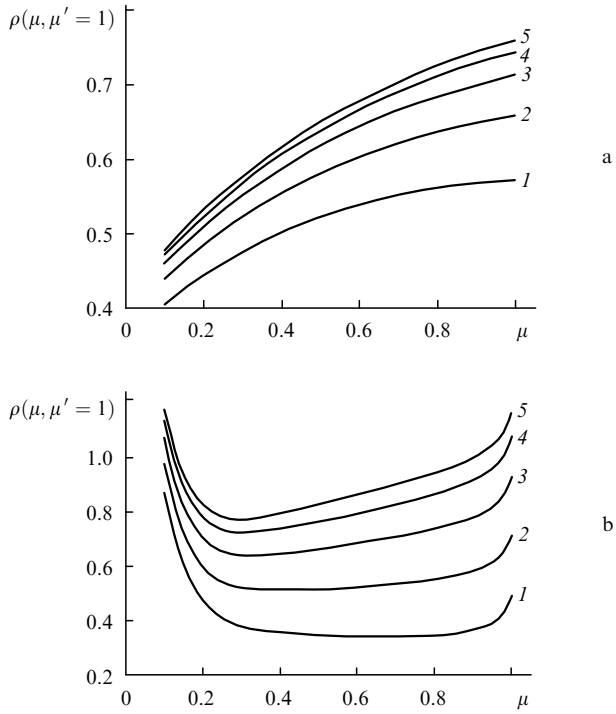

Figure 12. Luminance factors $\rho(\mu, \mu' = 1)$ of a layer formed by particles with $R_p = 0.199$ μm and $n_p = 1.05$ ($\lambda = 0.5$ μm) for $\eta = 625$ [curve (*1*)], 1250 [curve (*2*)], 2500 [curve (*3*)], 5000 [curve (*4*)], and 10000 [curve (*5*)]; $u = 0.0985$, $\tau_0 = 23.94$, $w = 0.001$ (a) and 0.5 (b).

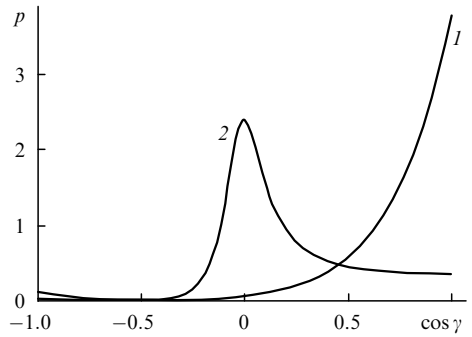

Figure 11. Phase functions of a unit volume of the medium formed by particles with $R_p = 0.199$ μm, $n_p = 1.05$ ($\lambda = 0.5$ μm) for $w = 0.001$ [curve (*1*)] and 0.5 [curve (*2*)].

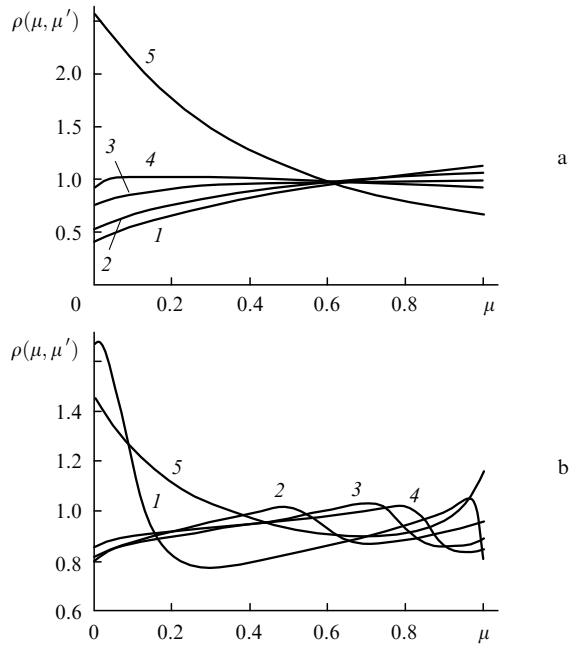

Figure 13. Angular dependences of the luminance factors $\rho(\mu, \mu')$ of a layer formed by particles with $R_p = 0.199$ μm, $n_p = 1.05$ ($\lambda = 0.5$ μm) and $\eta = 10000$ for $\mu' = 1$ [curve (*1*)], 0.838 [curve (*2*)], 0.659 [curve (*3*)], 0.557 [curve (*4*)], and 0.211 [curve (*5*)]; $u = 0.0985$, $\tau_{0l} = 239.4$, $\eta = 10000$, $w = 0.001$ (a) and 0.5 (b).

back-scattered radiation for different values of μ' for the same media. For low particle concentrations, the dependences are smooth and nearly linear for $\mu > 0.5$. For high concentrations, the presence of interference peaks leads to sharp dips in the angular dependence of the back-scattered radiation. If the peak in the phase function is not directed strictly at an angle of 90° (Fig. 14), the peak in the luminance factor is deviated from the strictly backward direction (Fig. 15).

5. Conclusions

We have developed a method for describing the propagation of radiation in layers of a close-packed medium formed by optically soft particles. It includes the Mie theory (for describing the parameters of single scattering), interference approximation (for describing the collective scattering effects), and the radiation transfer theory (for describing the light field in the multiple scattering mode).

A numerical calculation method based on the layer-doubling technique and spline approximation of the phase function approximation is proposed for solving the radiation transfer equation in a high-concentration layer.

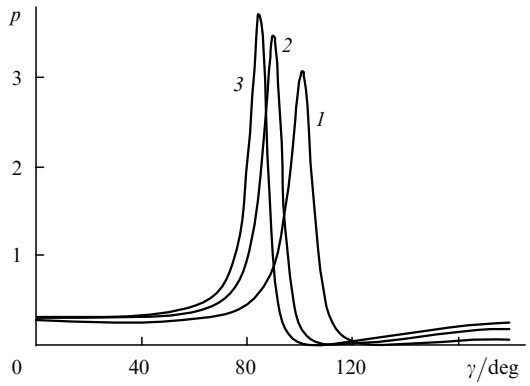

Figure 14. Phase functions of a unit volume of the medium formed by particles with $n_p = 1.05$ ($\lambda = 0.5$ μm) and $w = 0.6$ for $R_p = 0.19$ [curve (*1*)], 0.2072 [curve (*2*)], and 0.2172 μm [curve (*3*)].

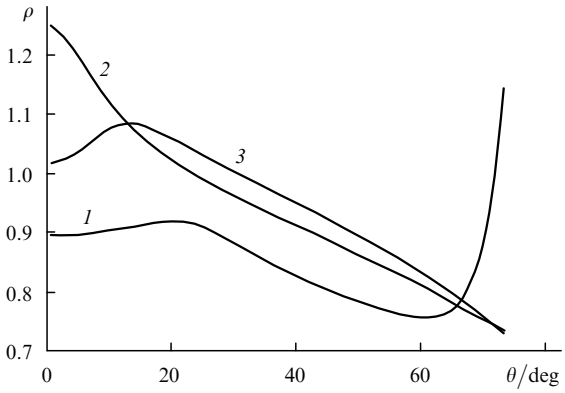

Figure 15. Angular dependences of the luminance factors $\rho(\theta, \theta' = 0)$ of a layer formed by particles with $n_p = 1.05$ ($\lambda = 0.5$ μm), $w = 0.6$ and $\eta = 10000$ for $R_p = 0.19$ [curve (*1*)], 0.2072 [curve (*2*)], and 0.2172 mm [curve (*3*)].

The variation of the angular structure of scattered radiation is analysed for an azimuth-symmetric illumination of the layer in a wide range of optical thicknesses. We have determined the salient features of the angular structure of the intensity of radiation scattered in the forward and backward semispheres in dispersed layers the phase function of whose unit volume has a typical interference peak at nonzero scattering angles. For normal illumination, this peak leads to the formation of a peak in the angular structure of radiation scattered by the layer in the strictly forward direction upon an increase in the optical thickness of the layer. This peak is smoothed out upon a transition to the thickness mode. The peak is blurred for a slanted illumination. Two peaks whose separation increases with the incidence angle can also be formed. For media in which the phase function for a unit volume has a peak at an angle of 90°, the peak formed in the strictly forward direction upon a normal incidence of radiation on the layer is accompanied by a peak in the strictly backward direction also. This peak is preserved upon an increase in the optical thickness of the layer.

References

1. Tiggelen B.A., Skipetrov S.E. (Eds). *Wave Scattering in Complex Media: From Theory to Applications* (Dordrecht: Kluwer Acad. Publ., 2003).
2. Twersky V. *J. Opt. Soc. Am.*, **52**, 145 (1962).
3. Ishimaru A. *Propagation and Scattering of Light in a Random Media* (New York: Academic Press, 1981).
4. Tsang L., Kong J.A., Shin R.T. *Theory of Microwave Remote Sensing* (New York: Wiley, 1985).
5. Ivanov A.P., Loiko V.A., Dick V.P. *Rasprostranenie sveta v plotnoupakovannykh dispersnykh sredakh* (Propagation of Light in Close-Packed Dispersive Media) (Minsk: Nauka i Tekhnika, 1988).
6. Dick V.P., Loiko V.A. *Liquid Crystals*, **28**, 1193 (2001).
7. Loiko V.A., Berdnik V.V. *Opt. Spektrosk.*, **100**, 1002 (2006).
8. Mischenko M.I. *J. Quantum Spectrosc. Radiat. Transfer*, **52**, 95 (1994).
9. Tsang L., Ishimaru A. *J. Opt. Soc. Am. A*, **2**, 1131 (1985).
10. Tsang L., Ding K.H., Shih S.E., Kong J.A. *J. Opt. Soc. Am. A*, **15**, 2660 (1998).
11. Loiko V.A., Berdnik V.V., Tiggelen B.A., Skipetrov S.E. (Eds) *Wave Scattering in Complex Media: From Theory to Applications* (Dordrecht: Kluwer Acad. Publ., 2003) p. 535.
12. Berdnik V.V., Loiko V.A. *J. Quantum Spectrosc. Radiat. Transfer*, **88**, 111 (2004).
13. Chandrasekhar S. *Radiative Transfer* (Oxford: Clarendon Press, 1950).
14. Van de Hulst H.C. *Multiple Light Scattering Tables, Formulas and Applications. V.1* (New York: Wiley, 1980).
15. Sobolev V.V. *Perenos luchistoi energii v atmosfere zvezd i planet* (Energy transport in Star and Planetary Atmosphere) (Moscow: Gostekhizdat, 1956).
16. Lenoble J. (Ed.) *Radiative Transfer in Scattering and Absorbing Atmospheres: Standard Computational Procedures* (Hampton: Deepak Publishing, 1985; Leningrad: Gidrometeoizdat, 1989).
17. Minin I.N. *Teoriya perenosa izlucheniya v atmosferakh planet* (Theory of Radiation Transport in Planetary Atmospheres) (Moscow: Nauka, 1983).
18. Bohren C.F., Huffman D.R. *Absorption and Scattering of Light by Small Particles* (New York: Wiley, 1983).
19. Deirmendjian D. *Electromagnetic Scattering on Spherical Polydispersions* (New York: American Elsevier, 1969).
20. Babenko V.A., Astafyeva L.G., Kuzmin V.N. *Electromagnetic Scattering in Disperse Media* (Berlin: Springer Praxis Publ., 2003).
21. Percus J.K., Yevick G.Y. *Phys. Rev.*, **110**, 1 (1958).
22. Ziman J.M. *Models of Disorder* (Cambridge: University Press, 1979).
23. Kuz'min V.L., Romanov V.P., Obraztsov E.P. *Opt. Spektros.*, **91**, 972 (2001).
24. Ishimaru A., Kuga Y. *J. Opt. Soc. Am.*, **72**, 1317 (1982).
25. Berdnik V.V., Loiko V.A. *J. Quantum Spectrosc. Radiat. Transfer*, **61**, 49 (1999).
26. Berdnik V.V., Mukhamedyarov R.D. *Opt. Spektrosk.*, **90**, 652 (2001).
27. Zav'yalov Yu.S., Kvasov B.I., Miroshnichenko V.L. *Metody Splain-funktsii* (Spline Function Methods) (Moscow: Nauka, 1980).
28. Amosov A.A., Dubinskii Yu.A., Kopchenova N.V. *Vychislitel'nye metody dlya inzhenerov* (Computational Techniques for Engineers) (Moscow: Vysshaya shkola, 1994).
29. Plass G.N., Kattawar G.W., Catchings F.F. *Appl. Opt.*, **12**, 314 (1973).
30. Wiscombe W.J. *J. Quantum Spectrosc. Radiat. Transfer*, **16**, 636 (1976).
31. Hunt G.E. *J. Quantum Spectrosc. Radiat. Transfer*, **11**, 309 (1971).
32. Loiko V.A., Molochko V.I. *Liquid Crystals*, **25**, 603 (1998).